ACS Photonics

Article

pubs.acs.org/journal/apchd5

Photonic Crystals for Enhanced Light Extraction from 2D Materials

Yasir J. Noori, Yameng Cao, Jonathan Roberts, Christopher Woodhead, Ramon Bernardo-Gavito, Peter Tovee, and Robert J. Young*

Department of Physics, Lancaster University, Lancaster, LA1 4YB, U.K.

ABSTRACT: In recent years, a range of two-dimensional transition metal dichalcogenides (TMDs) have been studied, and remarkable optical and electronic characteristics have been demonstrated. Furthermore, the weak interlayer van der Waals interaction allows TMDs to adapt to a range of substrates. Unfortunately, the photons emitted from these TMD monolayers are difficult to efficiently collect into simple optics, reducing the practicality of these materials. The realization of on-chip optical devices for quantum information applications requires structures that maximize optical extraction efficiency while also minimizing substrate loss. In this work we propose a photonic crystal cavity based on silicon rods that allows maximal spatial and spectral coupling between TMD monolayers and the cavity mode. Finite difference time domain simulations revealed that TMDs coupled to this type of cavity have highly directional emission toward the collection optics, as well as up to 400% enhancement in luminescence intensity, compared to monolayers on flat substrates. We consider realistic fabrication tolerances and discuss the extent of the achievable spatial alignment with the cavity mode field maxima.

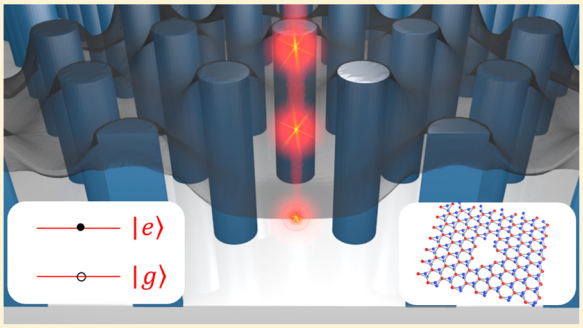

KEYWORDS: *transition metal dichalcogenides, molybdenum disulfide, extraction efficiency, photonic crystals, finite difference time domain*

Solid-state lighting has enabled a vast range of applications, making it one of the most important technologies of the 21st century, recently recognized by the Nobel Prize in Physics in 2014.[1] Modern fabrication techniques for solid-state devices have enabled the creation of quantum light sources, capable of producing single and entangled photons.[2,3] Quantum light sources provide a variety of unique applications, such as the ability to securely share information between two parties using quantum key distribution (QKD) protocols.[4] Commercially available QKD systems are handicapped by their large form factor, high cost, and nondeterministic generation of high-purity single photons, leaving them vulnerable to certain attacks.[5] Currently, there is a large drive to develop full QKD systems at the microscopic scale,[6] incorporating the aforementioned quantum light sources as their qubit generators. Other nascent applications of quantum light include beating the classical diffraction limit in quantum imaging,[7,8] reducing cell damage in the microscopy of biological systems,[9] random number generators,[10] high-resolution metrology,[11] and linear all-optical quantum computing.[12,13]

Existing implementations of single-photon sources, using atoms,[14,15] organic molecules,[16] nitrogen vacancies in diamond,[17] and semiconductor quantum dots,[18−20] often operate at cryogenic temperatures and are difficult to position control. This leads to unsolved scalability challenges, prohibiting widespread adoption of the technology. Recently, considerable interest has been given to single-photon sources based on two-dimensional (2D) direct-gap quantum emitters, such as monolayer transition metal dichalcogenides (TMDs). For example, single-photon sources based on molybdenum disulfide (MoS_2) and tungsten diselenide (WSe_2) have been demonstrated,[21,22] which operate at visible wavelengths, compatible with conventional silicon photodetectors. Furthermore, due to the large spin−orbit coupling,[23] it has been shown that pure spin states can be electrically controlled in these monolayers, as they are protected against decoherence by the spin-split valence band. Another desirable attribute of 2D quantum emitters, and possibly the most interesting, is their ability to be reliably transferred onto different substrates,[24] enabling integration into on-chip quantum photonic circuits. The current bottleneck for the application of this technology is the low optical absorption of a few percent that these monolayers exhibit. This severely limits the luminescence efficiency of light from these monolayers for potential optoelectronic implementations.[25] Existing approaches to circumnavigate this limitation are material specific, such as treatment of MoS_2 using organic superacid,[26] tunable Bragg mirrors for $MoSe_2$ and BN heterostructures,[27] and enhancement of MoS_2 luminescence via engineered plasmonic structures.[28,29] Therefore, a universal approach that offers light emission enhancement for all TMDs would prove advantageous to adapt nascent quantum technologies across a wide range of materials. One possible solution is to couple the TMD emitters to photonic crystal structures,[30] which tailors the emission properties to maximize light extraction.

Received: October 11, 2016
Published: November 14, 2016

DOI: 10.1021/acsphotonics.6b00779
ACS Photonics 2016, 3, 2515−2520

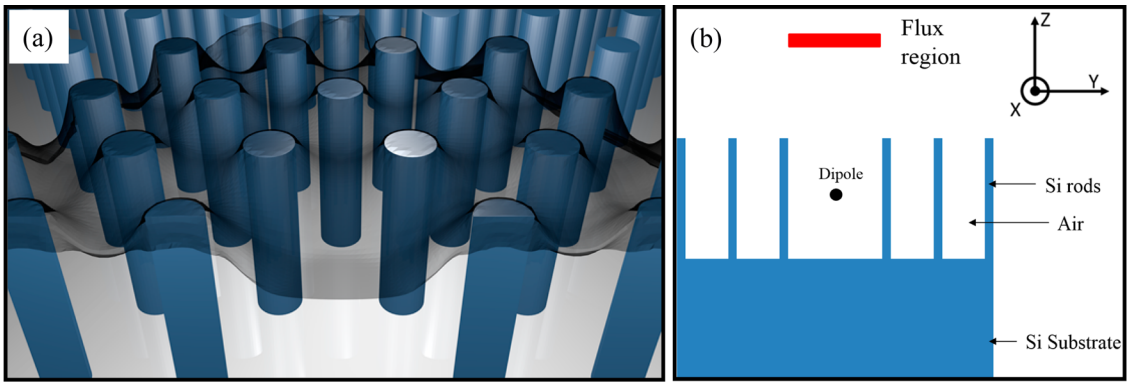

Figure 1. (a) Cross-sectional illustration of a silicon rod photonic crystal cavity with a monolayer transferred on top of it. (b) Cross-sectional schematic diagram of the 3D simulated cavity.

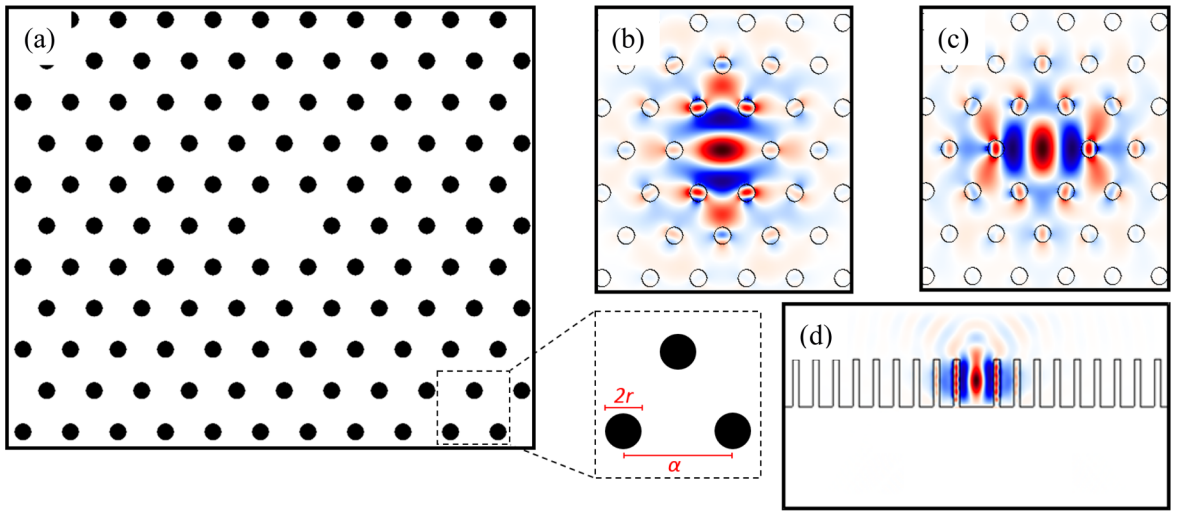

Figure 2. (a) An $x-y$ cross section of the simulated photonic crystal cavity structure through the rod structure. 3D FDTD simulation of the photonic cavity mode showing time slice images of the confined (b) E_x and (c) E_y field components. (d) Cross section of the E_y field component within the microcavity. Red (blue) represents positive (negative) components of the electric field.

Monolayer−cavity coupling has been demonstrated recently using an air-bridge photonic crystal. Previous work has shown lasing and an enhancement in the spontaneous emission rate for light emitted from 2D materials.[31−34] This method, in principle, offers advantages including contact fabrication and minimized vertical mode loss via the refractive index differential. However, it also results in the cavity's resonant emission being confined within the high-index slab, rather than directionally coupled out of the plane of the 2D material, limiting the extraction efficiency. We will show that the rod-type structure proposed here directly enhances the extraction efficiency via a vertically distributed cavity mode. In the present work, we consider a monolayer embedded in a photonic crystal consisting of silicon rods arranged in a triangular lattice with a missing rod from the lattice constituting a resonant cavity, as shown in Figure 1a. The important figure of merit here is the light extraction enhancement ratio η_e, defined as

$$\eta_e = P_{cav}/P_0 \quad (1)$$

where P_{cav} corresponds to the power collected from a monolayer coupled to the photonic cavity and P_0 corresponds to the reference power measured for a monolayer exfoliated on top of a silicon substrate.

Spatial coupling between the cavity and the monolayer will be achieved by suspending the monolayer over the rods; Figure 1a illustrates this concept. With sufficient lattice separation, the cavity region, consisting of a single missing rod, should allow the suspended flake to sag[35] such that the flake's topological minimum spatially matches the cavity mode's antinode. Alignment in both position and energy leads to a modification in the local density of optical states such that the spontaneous emission rate can be improved via the Purcell effect, which is proportional to the field amplitude squared. Suspension-induced sag will also result in mechanical strain, which could help to promote the synthesis of defect-trapped excitons.[36]

METHODS

The cavity design we propose consists of a triangular array of rods surrounded by air for optimum index contrast. The rods have a refractive index of 3.9, corresponding to the refractive index of silicon at the MoS_2 monolayer emission wavelength of approximately 660 nm. We consider the MoS_2 emission wavelength due to its high neutral and charged exciton binding energies, which makes it a promising candidate for room-temperature quantum light sources. Nonetheless, our design is universal, as the normalized parameters may be scaled and adjusted to match any light-emitting TMD. Three-dimensional

DOI: 10.1021/acsphotonics.6b00779
ACS Photonics 2016, 3, 2515−2520

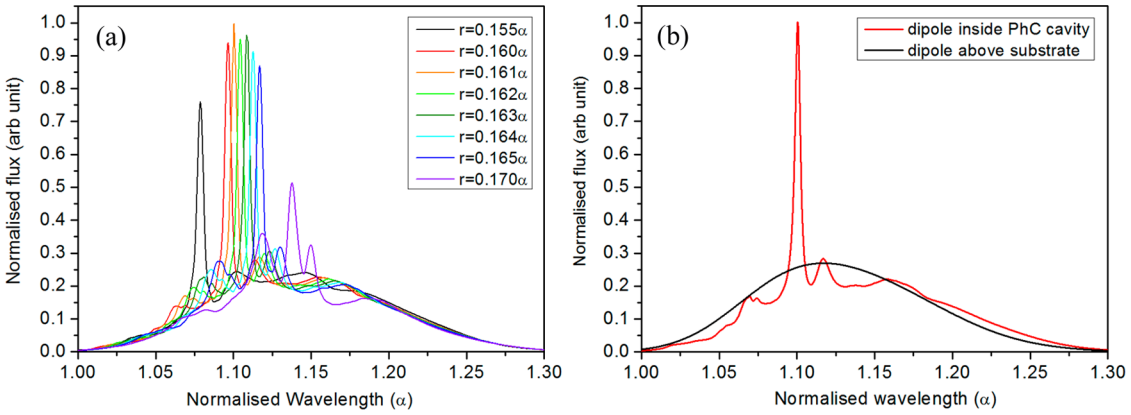

Figure 3. (a) Enhancement spectra for rods with a radius ranging from 0.155α to 0.170α. (b) Normalized flux spectrum for a crystal with $r = 0.161\alpha$, compared with the emission from a source on a bulk substrate.

finite difference time domain (FDTD) simulations of the dipole cavity modes of this rod-type photonic crystal cavity were performed using open-source software written by Oskooi et al.[37] In all the simulations performed, perfectly matched layers were incorporated at the boundaries of the simulation domain to avoid unnecessary reflections of light. The rods' radii were varied between 0.155α and 0.170α (where α is the lattice constant) to obtain the optimum radius in which the Q-factor and the corresponding extraction enhancement factor η_e were maximized. Unsurprisingly, the rod's height also influences photonic confinement, if the rods are too short, the mode shape can extend into the air above the photonic crystal. Subsequently, the reduction of the spatial interface between the mode and the rods reduces the light extraction ratio. Conversely, if the rods are too tall, higher order modes and propagating modes can form within the structure. Furthermore, high aspect ratio rods require complex etching methods to achieve the required degree of anisotropy. Previous work has shown that the maximum gap size for a square rod-type photonic crystal is calculated for rod heights of approximately 2.3α, corresponding to approximately 2 cavity mode wavelengths.[38] In our work, we found that this also applies to triangular lattices. Therefore, the rods' height was fixed to 2.3α in all simulation runs.

Compared to air-bridge photonic crystal structures,[31−34] rod-type photonic crystals have a lower dielectric−air ratio in their lattice, effectively suppressing dielectric absorption of the luminescence. This makes our cavity structure less influential to light absorption issues. Hence, in all simulations the dielectric constant for the silicon pillars was chosen to be real; that is, any absorption due to the dielectric material within the pillars was ignored.

RESULTS AND DISCUSSION

Using 2D plane wave expansion (PWE)[39] simulation methods with the triangular lattice photonic crystal shown in Figure 2a, we obtained a photonic band gap for transverse electric (TE)-like modes at normalized wavelengths of $\lambda = 1.05-1.17\alpha$. Subsequently, a defect was created by omitting a single rod from the lattice in a location surrounded by six or more lattice points. For rods with a radius of 0.161α, this creates a localized state at a normalized wavelength of 1.11α, resulting in a light-trapping cavity.

The simulation was run initially with an E_x-polarized source placed exactly in the center of the cavity. A broadband source was set up for initial identification of the confined mode wavelength. An FDTD time slice of the spatial distribution of the cavity mode in the vicinity of the defect for the E_x mode is shown in Figure 2b. The second component of the TE mode in the plane of the photonic crystal lattice, the E_y mode, was simulated, and the designed cavity was shown to have a confined mode as shown in Figure 2c. It is clear from the figure that the shape of the defect-localized mode for the cavity exhibits the character of the underlying hexagonal lattice. Results for the resonance wavelength of the cavity and its Q-factor were obtained using the harmonic inversion solving technique.[40] The Q-factor was measured to be more than 300 when the full photonic crystal structure was simulated with 3D FDTD. The relatively low Q-factor is to be expected due to radiative mode loss in the vertical direction.

Modeling photonic crystal cavities using periodic dielectric rods has been reported previously.[41] A square lattice structure of dielectric rods with radii of 0.2α was used to realize a transverse magnetic mode cavity, producing a cavity mode wavelength of $\lambda = 2.6\alpha$. The main drawback that this design suffers from is the small radius requirement of the dielectric rods for a predefined cavity mode wavelength. For example, enhancing light from MoS_2 monolayers at a wavelength of 660 nm would require the lattice constant to be as small as 250 nm and the rods' diameters to be 50 nm. This renders the fabrication of such cavities a significant challenge for mode wavelengths in the visible regime, even with state-of-the-art e-beam lithography techniques and highly tuned anisotropic etching recipes. Using our proposed hexagonal array design of dielectric rods, the lattice constant and rods' radius are approximately 595 and 95 nm, respectively, alleviating some of the fabrication challenges. The practical properties of this design make it more attractive to study in the application of monolayers for optoelectronic devices. In addition, the large diameter size of the photonic crystal rods, which distinguishes our design, allows easier transfer of 2D materials on top of the rod structures. This is due to the improved surface contact between the top surface of the rods and the 2D flakes, leading to higher adhesion.

To measure the improved extraction efficiency of light, we mimic an objective lens with a numerical aperture of 0.65 and a flux region of area $23\alpha^2$ set up above the cavity, collecting vertically radiated light at a height of 2α above the top of the rods. We obtained the extraction ratio, η_e, by measuring the transmitted power through such a flux region for a cavity-

DOI: 10.1021/acsphotonics.6b00779
ACS Photonics 2016, 3, 2515−2520

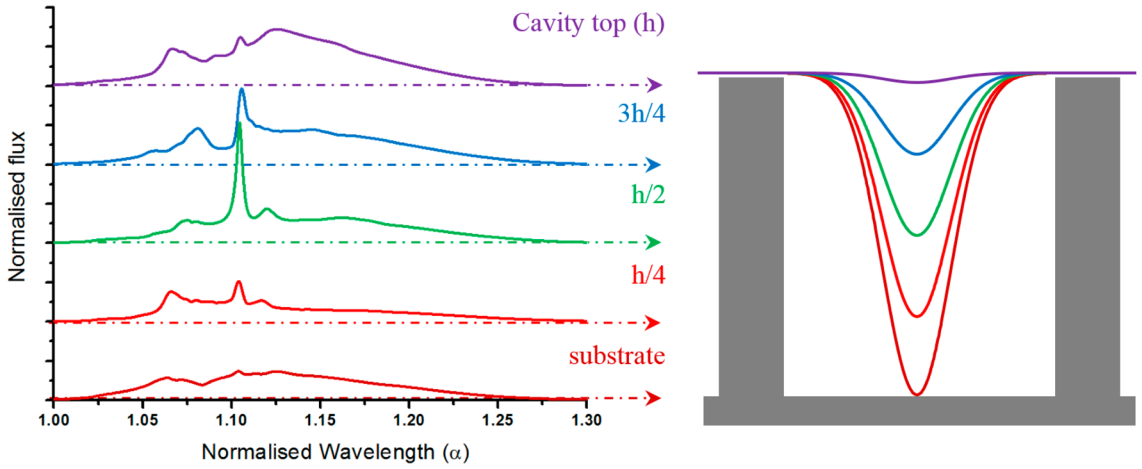

Figure 4. Comparison of the flux spectra for emission from the cavity as the dipole position inside the cavity is varied along the *z*-axis. The drawing on the right illustrates the degrees of bowing of the 2D material from the surface of the structure into the cavity for each of the cases shown on the left.

coupled emitter and the same emitter placed directly on a substrate. The comparison was made between a source within the 3D modeled cavity and a source above a silicon slab, where the dipole represents a 2D flake suspended on the structure as shown in Figure 1b and a flake exfoliated on a silicon substrate, respectively.

Modeling of the collected flux as a function of different photonic crystal rod radii, *r*, was carried out in order to investigate the effect on the enhancement of the collected light due to nonuniformities in the fabrication of the structures. Figure 3a illustrates the collected flux spectrum as the rods' radius is changed from 0.155α to 0.170α. The results show maximum enhancement in the light extraction efficiency when the rods' radius is 0.161α. As the rods' radius deviates from this value, the enhancement starts to decrease. It is important to notice that reducing the radius of the rods blue-shifts the cavity modes at a constant rate between 0.155α and 0.170α. This is anticipated, as the relationships between cell diameters and the resonance wavelength was modeled in many photonic crystal cavity studies.[42]

Figure 3b plots a comparison between the obtained flux for an emitter inside our proposed cavity structure with rods of radius 0.161α and for an emitter placed directly above a flat substrate. When the source is placed directly on top of the substrate, a Gaussian curve is obtained, which corresponds to the input dipole source emission wavelength and bandwidth as shown by the black curve in Figure 3b. On the other hand, placing the dipole within the vicinity of the cavity results in an enhancement in the recorded flux, as shown by the red curve. This is attributed to radiation modes from the cavity leaking vertically toward the flux region. For $\lambda = 1.104\alpha$, the light extraction ratio, η_e, was observed to be approximately 400%.

While strain due to the suspension of 2D monolayer flakes can promote the creation of light-emitting defects,[36] the exact position of the defect in the vertical direction inside the cavity cannot be easily anticipated without setting up simulations using finite element methods. Hence, we modeled the change obtained in the emitted spectrum as the monolayer region is suspended above the cavity at different heights for a rod radius of 0.161α. Figure 4 shows simulation results of different flux spectra collected as the position of the dipole emitter is changed along the *z*-axis from the bottom of the cavity to the top. Maximum Purcell enhancement should be achieved when the source is spatially aligned with the cavity mode's electric field maximum; this occurs at the center of the cavity, as shown in Figure 2d. It is clear from Figure 4 that the maximum enhancement is achieved when the emitter is placed at a vertical position equal to half the height of the rods, one wavelength above the substrate, where the cavity's mode field is maximum. Enhancement decreases when the source is moved toward the top of the rods due to reduced spatial coupling between the emitter and the cavity mode, while also coupling to radiative modes. The same applies when the emitter is placed near the bottom of the cavity, where coupling to substrate-mediated leaky modes is dominant.

It is worth mentioning that L3 cavities that are made by omitting three rods from the photonic crystal lattice exhibit similar confinement characteristics. Preliminary results found that quality factors of more than 100 are achievable, with extraction efficiencies close to 300%. Large cavities such as L3 and L5 can further promote the bowing of 2D materials inside the cavity, improving coupling of the emitter to the cavity mode.

The collection efficiency of emission from the cavity could be further improved by adding a solid immersion lens (SIL) on top of the photonic crystal structure.[43] Glass SILs can be reliably positioned with micrometer-scale accuracy. Such SILs have been reported to achieve over 3 times enhancement in the extraction ratio, while SILs made of other materials such as GaAs can achieve over 10 times enhancement.[44] The second advantage SILs could offer in our proposed photonic structure is the enhanced vertical confinement due to total internal reflection inside the cavity. By adding a slab of a similar refractive index to that of glass, FDTD simulations showed a 4-fold enhancement in the cavity's *Q*-factor with the SIL in place. Combining our photonic crystal structure with a SIL could potentially enhance the extraction ratio of light by over 40 times. This makes combining a SIL with our proposed rod-type photonic crystal cavity a promising method for efficient extraction of light from 2D monolayer light emitters such as TMDs.

CONCLUSION

In this work we proposed a scheme for coupling two-dimensional transition metal dichalcogenide monolayers to a

DOI: 10.1021/acsphotonics.6b00779
ACS Photonics 2016, 3, 2515−2520

rod-type photonic crystal cavity. The proposed photonic cavity structure can be scaled to couple to a wide range of TMD monolayers' emission wavelengths. While the simulated cavity in this work was made of silicon rods, the design is invariant when gallium arsenide or materials of similar refractive indices are used. By transferring a monolayer on top of our proposed cavity structure, the sagging of the monolayer within the cavity allows coupling between the cavity mode and the TMD emitter. We compared the extraction ratio of light from a monolayer coupled to our cavity with a case in which the monolayer is transferred onto a bulk substrate. We found that our structure can provide up to 4 times enhancement in the extraction ratio. We performed a series of simulations to show how susceptible the design is to changes in the rod radius and the vertical position of the light emitter inside the cavity. Simulations were carried out for rod radii between 0.155α and 0.170α, where maximum enhancement was achieved for a radius of 0.161α. The enhancement decreases slowly as r is changed. The enhancement in the extracted light is also affected by the vertical position of the emitter within the cavity along the z-axis. Optimum enhancement is achieved when the dipole is at the center of the cavity, where the electric field is at a maximum. This allows the greatest coupling to the emitter, whereas the enhancement decreases gradually as it reaches the top of the cavity. Finally, we discussed how solid immersion lenses placed on top of the cavity could be used to enhance vertical confinement of the cavity mode within the vicinity of the cavity, increasing the total light extraction ratio to over 40 times. This enhancement is a strong step forward toward improved extraction efficiency of quantum and classical light from TMD-based devices.

AUTHOR INFORMATION

Corresponding Author

*E-mail: r.j.young@lancaster.ac.uk.

ORCID

Robert J. Young: 0000-0002-5719-2205

Notes

The authors declare no competing financial interest.

ACKNOWLEDGMENTS

This work was supported by the Royal Society through a University Research Fellowship (UF110555) held by R.J.Y. This material is based upon work supported by the Air Force Office of Scientific Research under award number FA9550-16-1-0276. This work was also supported by grants from The Engineering and Physical Sciences Research Council in the UK (grant numbers EP/K50421X/1 and EP/L01548X/1).

REFERENCES

(1) The Nobel Foundation. The Nobel Prize in Physics 2014. https://www.nobelprize.org/nobel_prizes/physics/laureates/2014/ (accessed 10/10/2016).

(2) Stevenson, R. M.; Young, R. J.; Atkinson, P.; Cooper, K.; Ritchie, D. A.; Shields, A. J. A semiconductor source of triggered entangled photon pairs. *Nature* **2005**, *439*, 179−182.

(3) Zhang, J.; Wildmann, J. S.; Ding, F.; Trotta, R.; Huo, Y.; Zallo, E.; Huber, D.; Rastelli, A.; Schmidt, O. G. High yield and ultrafast sources of electrically triggered entangled-photon pairs based on strain-tunable quantum dots. *Nat. Commun.* **2015**, *6*, 10067.

(4) Bennett, C. H.; Brassard, G. Quantum cryptography: public key distribution and coin tossing. *Proceedings of IEEE International Conference on Computers, Systems and Signal Processing*; 1987; p 175.

(5) Brassard, G.; Lutkenhaus, N.; Mor, T.; Sanders, B. C. Limitations on practical quantum cryptography. *Phys. Rev. Lett.* **2000**, *85*, 1330−1333.

(6) Sibson, P.; Erven, C.; Godfrey, M.; Miki, S.; Yamashita, T.; Fujiwara, M.; Sasaki, M.; Terai, H.; Tanner, M. G.; Natarajan, C. M.; Hadfield, R. H.; O'Brien, J. L.; Thompson, M. G. *Chip-based quantum key distribution*. 2015 arXiv:1509.00768.

(7) Boto, N.; Kok, P.; Abrams, D. S.; Braunstein, S. L.; Williams, C. P.; Dowling, J. P. Quantum interferometric optical lithography: exploiting entanglement to beat the diffraction limit. *Phys. Rev. Lett.* **2000**, *85*, 2733−2736.

(8) Stevenson, R. M.; Hudson, A. J.; Young, R. J.; Atkinson, P.; Cooper, K.; Ritchie, D. A.; Shields, A. J. Biphoton interference with quantum dot entangled light source. *Opt. Express* **2007**, *15*, 6507−6512.

(9) Denk, W.; Strickler, J. H.; Webb, W. W. Two-photon laser scanning fluorescence microscopy. *Science* **1990**, *248*, 73−76.

(10) Ma, H.; Wang, S.; Zhang, D.; Chang, J.; Ji, L.; Hou, Y.; Wu, L. A random number generator based on quantum entangled photon pairs. *Chin. Phys. Lett.* **2004**, *21*, 1961−1964.

(11) Motes, K. R.; Olson, J. P.; Rabeaux, E. J.; Dowling, J. P.; Olson, S. J.; Rohde, P. P. Linear Optical quantum metrology with single photons: exploiting spontaneously generated entanglement to beat the shot-noise limit. *Phys. Rev. Lett.* **2015**, *114*, 170802.

(12) O'Brien, J. L. Optical quantum computing. *Science* **2007**, *318*, 1567−1570.

(13) Knill, E.; Laflamme, R.; Milburn, G. J. A scheme for efficient quantum computation with linear optics. *Nature* **2001**, *409*, 46−52.

(14) Kimble, H. J.; Dagenais, M.; Mandel, L. Photon antibunching in resonance fluorescence. *Phys. Rev. Lett.* **1977**, *39*, 691−695.

(15) Diedrich, F.; Walther, H. Nonclassical radiation of a single stored ion. *Phys. Rev. Lett.* **1987**, *58*, 203−206.

(16) Lounis, B.; Moerner, W. E. Single photons on demand from a single molecule at room temperature. *Nature* **2000**, *407*, 491−493.

(17) Kurtsiefer, C.; Mayer, S.; Zarda, P.; Weinfurter, H. Stable solid-state source of single photons. *Phys. Rev. Lett.* **2000**, *85*, 290−293.

(18) Tomic, S.; Pal, J.; Migilorato, M. A.; Young, R. J.; Vukmirovic, N. Visible spectrum quantum light sources based on $In_xGa_{1-x}N$/GaN quantum dots. *ACS Photonics* **2015**, *2*, 958−963.

(19) Santori, C.; Pelton, M.; Solomon, G.; Dale, Y.; Yamamoto, Y. Triggered single photons for a quantum dot. *Phys. Rev. Lett.* **2001**, *86*, 1502−1505.

(20) Holmes, M.; Choi, K.; Kako, S.; Arita, M.; Arakawa, Y. Room-temperature triggered single photon emission from a III-Nitride site-controlled nanowire quantum dot. *Nano Lett.* **2014**, *14*, 982−986.

(21) Berraquero, C. P.; Barbone, M.; Kara, D. M.; Chen, X.; Ilya, G.; Yoon, D.; Ott, A. K.; Beitner, J.; Watanabe, K.; Taniguchi, T.; Ferrari, A. C.; Atature, M. *Atomically thin quantum light emitting diodes*. 2016 arXiv:1603.08795.

(22) Chakraborty, C.; Kinnischtzke, L.; Goodfellow, K. M.; Beams, R.; Vamivakas, A. N. Voltage-controlled quantum light from an atomically thin semiconductor. *Nat. Nanotechnol.* **2015**, *10*, 507−511.

(23) Kormanyos, A.; Zolyomi, V.; Drummond, N. D.; Burkard, G. Spin-orbit coupling, quantum dots, and qubits in monolayer transition metal dichalcogenides. *Phys. Rev. X* **2014**, *4*, 011034.

(24) Castellanos-Gomez, A.; Buscema, M.; Molenaar, R.; Singh, V.; Janssen, L.; Van der Zant, H. S. J.; Steele, G. A. Deterministic transfer of two-dimensional materials by all-dry viscoelastic stamping. *2D Mater.* **2014**, *1*, 011002.

(25) Paton, K. R.; Coleman, J. N. *Relating the opical absorption coefficient of nanosheet dispersion to the intrinsic monolayer absorption*. 2015 arXiv:1511.04410.

(26) Amani, M.; Lien, D. H.; Kiriya, D.; Xiao, J.; Azcatl, A.; Noh, J.; Madhvapathy, S. R.; Addou, R.; KC, S.; Dubey, M.; Cho, K.; Wallace, R. M.; Lee, S. C.; He, J. H.; Ager, J. W., III; Zhang, X.; Yablonovitch, E.; Javey, A. Near-unity photoluminescence quantum yield in MoS_2. *Science* **2015**, *4*, 1065−1068.

(27) Dufferwiel, S.; Schwarz, S.; Withers, F.; Trichet, A. A. P.; Li, F.; Sich, M.; Del Pozo-Zamudio, O.; Clark, C.; Nalitov, A.; Solnyshkov, D.

DOI: 10.1021/acsphotonics.6b00779
ACS Photonics 2016, 3, 2515−2520

D.; Malpuech, G.; Novoselov, K. S.; Smith, J. M.; Skolnick, M. S.; Krizhanovskii, D. N.; Tartakovskii, A. I. Exciton-polaritons in van der Waals heterostructures embedded in tunable microcavities. *Nat. Commun.* **2015**, *6*, 9579.
(28) Lee, K. C. J.; Chen, Y.; Lin, H.; Cheng, C.; Chen, P.; Wu, T.; Shih, M.; Wei, K.; Li, L.; Chang, C. Plasmonic gold nanorods coverage influence on enhancement of the photoluminescence of two-dimensional MoS2 monolayer. *Sci. Rep.* **2015**, *5*, 16374.
(29) Butun, S.; Tongay, S.; Aydin, K. Enhanced light emission from large area monolayers MoS_2 using plasmonic nanodisc arrays. *Nano Lett.* **2015**, *4*, 2700−2704.
(30) Yablonovitch, E. Inhibited spontaneous emission in solid-state physics and electronics. *Phys. Rev. Lett.* **1987**, *58*, 2059−2062.
(31) Wu, S.; Buckley, S.; Jones, A. M.; Ross, J. S.; Ghimire, N. J.; Yan, J.; Mandrus, D. G.; Yao, W.; Hatami, F.; Vuckovic, J.; Majumdar, A.; Xu, X. Control of two-dimensional excitonic light emission via photonic crystal. *2D Mater.* **2014**, *1*, 011001.
(32) Gan, X.; Gao, Y.; Mak, K. F.; Yao, X.; Shiue, R.; Van der Zande, A.; Trusheim, M. E.; Hatami, F.; Heinz, T. F.; Hone, J.; Englund, D. Controlling the spontaneous emission rate of monolayer MoS_2 in a photonic crystal nanocavity. *Appl. Phys. Lett.* **2013**, *103*, 181119.
(33) Ye, Y.; Wong, Z. J.; Lu, X.; Ni, X.; Zhu, H.; Chen, X.; Wang, Y.; Zhang, X. Monolayer excitonic laser. *Nat. Photonics* **2015**, *9*, 733−737.
(34) Wu, S.; Buckley, S.; Schaibley, J. R.; Feng, L.; Yan, J.; Mandrus, D. G.; Hatami, F.; Yao, W.; Vuckovic, J.; Majumdar, A.; Xu, X. Monolayer semiconductor nanocavity laser with ultralow thresholds. *Nature* **2015**, *520*, 69−72.
(35) Kay, N. D.; Robinson, B. J.; Fal'ko, V. I.; Novoselov, K. S.; Kolosov, O. V. Electromechanical sending of substrate charge hidden under atomic 2D crystals. *Nano Lett.* **2014**, *14* (6), 3400−3404.
(36) Lin, Z.; Carvalho, B. R.; Kahn, E.; Lv, R.; Rai, R.; Terrones, H.; Pimenta, M. A.; Terrones, M. Defect engineering of two-dimensional transition metal dichalcogenides. *2D Mater.* **2016**, *3*, 022002.
(37) Oskooi, A. F.; Roundy, D.; Ibanescu, M.; Bermel, P.; Joannopoulos, J. D.; Johnson, S. Meep: a flexible free-software package for electromagnetic simulations by the FDTD method. *Comput. Phys. Commun.* **2010**, *181*, 687−702.
(38) Johnson, S. G.; Fan, S.; Villeneuve, P. R.; Joannopoulos, J. D. Guided modes in photonic crystal slabs. *Phys. Rev. B: Condens. Matter Mater. Phys.* **1999**, *60*, 5751−5758.
(39) Prather, D. W.; Shi, S.; Sharkawy, A.; Murakowski, J.; Schneider, G. J.*Photonic Crystals; Theory, Applications and Fabrication*; Wiley Series in Pure and Applied Optics; 2009; pp 66−108.
(40) Mandelshtam, V. A.; Taylor, H. S. Harmonic inversion of time signals and its applications. *J. Chem. Phys.* **1997**, *107*, 6756−6769.
(41) Villeneuve, P. R.; Fan, S.; Joannopoulos, J. D. Microcavities in photonic crystals: mode symmetry, tenability and coupling efficiency. *Phys. Rev. B: Condens. Matter Mater. Phys.* **1996**, *54*, 7837−7842.
(42) Chengcheng, G.; Zhang, Y.; Du, J.; Xia, J.; Wang, J. Experimental demonstration of analog signal transmission in a silicon photonic crystal L3 resonator. *Opt. Express* **2015**, *23*, 13916−13923.
(43) Woodhead, C. S.; Roberts, J.; Noori, Y. J.; Cao, Y.; Bernardo-Gavito, R.; Tovee, P.; Kozikov, A.; Novoselov, K.; Young, R. J. Light extraction from 2D materials using liquid formed micro-lenses. 2016 arXiv:1607.05025.
(44) Serrels, K. A.; Ramsay, E.; Dalgarno, P. A.; Gerardot, B. D.; O'Connor, J. A.; Hadfield, R. H.; Warburton, R. J.; Reid, D. T. Solid immersion lens applications for nanophotonic devices. *J. Nanophotonics* **2008**, *2*, 021854.

DOI: 10.1021/acsphotonics.6b00779
ACS Photonics 2016, 3, 2515−2520